整・災外 53：1053−1061，2010

特集 脊椎インストゥルメンテーションのリスクとベネフィット

プレートを併用した頚椎広範囲前方除圧固定手術における留意点

大川 淳* 川端茂徳 加藤 剛
富澤将司 榎本光裕 四宮謙一

要旨：前方プレートの使用で，術直後であっても厳密な頚椎安静は不要となり，周術期の急性呼吸不全は減少した。また，頚椎カラー程度の外固定の併用で術後早期から起立歩行が開始可能となった。プレートには，スクリューとの間に動きがない constrained type と，上下あるいは回旋の動きをわずかに許容しつつ，抜去される方向には動かない semi-constrained type があり，最近では semi-constrained type での成績が良いという報告が多い。しかし，プレートによる内固定といっても絶対的な固定力が即時に得られるわけではない。3椎間以上の広範囲前方除圧固定術40例を対象として，周術期の合併症に関して調査したところ，移植腓骨の転位が2例，母床椎体骨折が2例，スクリュー突出単独が3例の計7例（17.5%）に再建合併症がみられた。頚椎の前弯が強いことが危険因子と考えられたが，移植骨が完全に脱転する前に棘突起ワイヤリングを追加することで対処可能であった。

はじめに

圧迫性頚髄症の手術治療は，脊髄圧迫の除去を目的として行われる。頚椎の不安定性が併存する場合に固定術が追加されるが，不安定性がなくても局所の動きをなくす方が神経回復にはよいとして，固定術が併用されることもある。頚椎の骨性固定を意図したときには，かつては前方固定術しか方法がなかったが，最近のインストゥルメンテーションの進歩により後方からの椎弓形成術にも固定術を組み合わせることが可能になった。

ただ，すべての圧迫性脊髄症が後方除圧固定術で対処できるわけではなく，頚椎後縦靱帯骨化症（OPLL）で骨化が厚く狭窄率が60%を超える場合や嘴状に局所突出がみられる場合，横断面において偏在性の場合には，広範囲前方除圧固定術の適応となる[1)2)]。広範囲前方除圧固定術では脊髄の前方に位置する骨化を浮上させるか，あるいは摘出することで脊髄を原位置に戻すことが可能である。また，頚椎症性脊髄症（CSM）においても，後弯が限界を超えると前方法の成績が良いことが報告されている[3)]。

こうしたことから，頚髄症の一部の症例において広範囲前方除圧固定術の必要性があり[4)]，ハローベストを利用した広範囲前方除圧固定術では良好な術後成績が報告されている。特に，池永ら[5)]は4椎間以上の118例において移植骨の脱転はなかったとして，すばらしい成績を報告している。しかし，ハローベストには，術直後の後咽頭腔の腫脹（図1）による急性呼吸不全にも気管挿

* Atsushi OKAWA et al，東京医科歯科大学大学院医歯学総合研究科，整形外科

Complication of cervical corpectomy and fusion with plate fixation

Key words：Anterior cervical corpectomy and fusion, Reconstruction failure, Anterior cervical plate

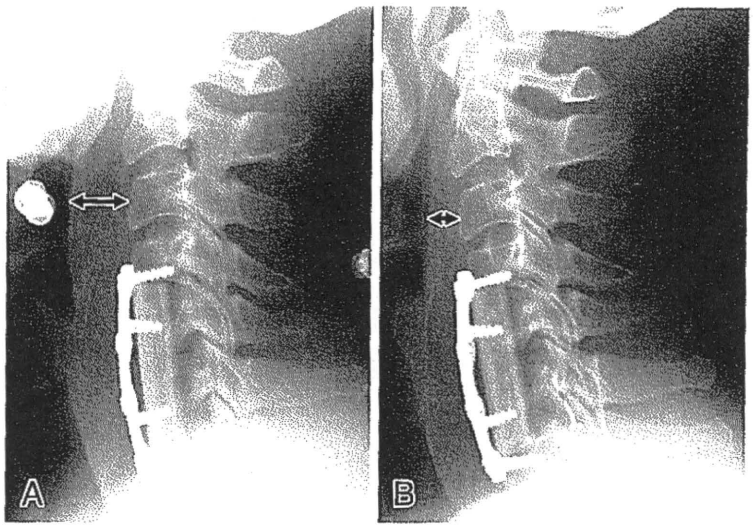

術後3日　　術後14日

図 1　術直後の後咽頭腔の腫脹

40歳男性のOPLLに対して，プレートを使用したC4-7椎体亜全摘前方除圧固定術を施行した。術後3日の頚椎X線側面像では，第3椎体高位での軟部腫脹が目立つ（A)。プレートがなくても同様の腫脹は発生し，急性の吸気困難となることがある。腫脹は時間がたてば自然軽快するので，初期数日の呼吸管理が重要である(B)。ハローベストでは，再挿管が困難なことが多いが，プレート固定であれば頚椎の伸展も可能である。

管による迅速な対処がしにくいこと，骨癒合まで2〜3カ月間にわたり装着を必要とすることなどの問題点があり，次第に前方プレートが利用されるようになった。

前方プレートの使用で，術直後であっても厳密な頚椎安静は不要となり，周術期の急性呼吸不全は減少した。また，頚椎カラー程度の外固定の併用で術後早期から起立歩行が開始可能となった。しかし，プレートによる内固定といっても絶対的な固定力が即時に得られるわけではない。Sasso[6]はプレートを併用した前方除圧固定術中，術後早期の再建合併症が2椎体切除では33例中2例であったものが，3椎体切除では7例中5例（71%）にみられたとしている。Daubs[7]は，複数椎体切除後の再建をメッシュケージとプレートで行った場合に，術後12週間以内に8例中6例が再建合併症を生じたと報告している。これらの報告はいずれもconstrained typeのプレートを用いたものであるが，再建合併症をできるだけ減らすためにはプレートの種類に限らず，いくつかの注意が必要と考えられる。本稿では，プレートを併用した頚椎広範囲前方除圧固定術における留意点について述べる。

Ⅰ．手術適応と術前準備

広範囲前方除圧固定術の上下方向の到達可能範囲は，C2下縁から1cm程度が上限で，胸骨縦割をしなければ通常T1上縁が無難であろう。厚い骨化（狭窄率60%以上）や嘴状の骨化，横断面で偏在する骨化を持つOPLLや後弯を形成するCSM・筋萎縮症が適応である。頚椎全体の前弯が保たれている場合には，後方からの除圧が基本である。また，頚椎症で広範囲にわたり除圧と固定が必要と考えられる場合には，椎体高位の除圧は不要であることがほとんどなので，椎間部のみを除圧する多椎間前方固定術を行う。

術前には患者の全身状態のチェックが重要であり，特に呼吸機能低下は術後の後咽頭腔の腫脹が

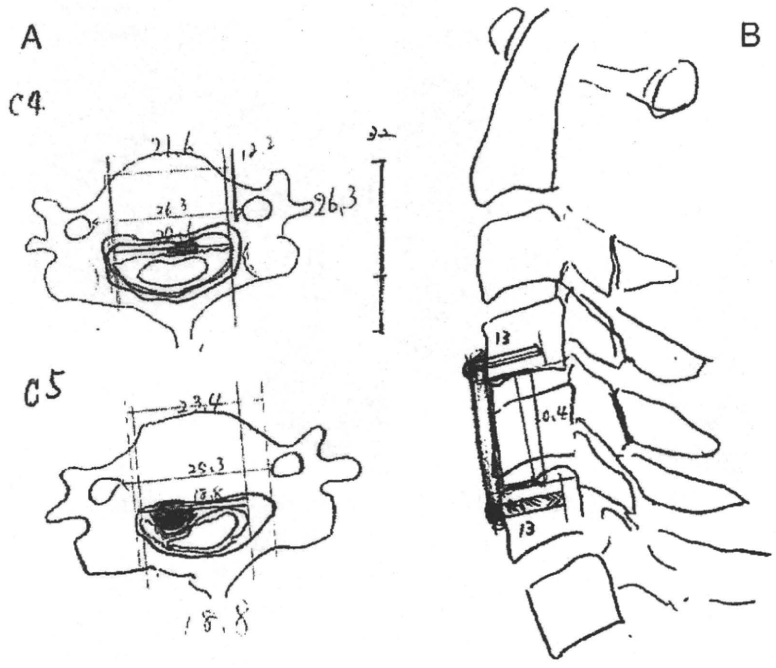

図 2　実際の paper surgery
C4-6 の前方除圧固定を予定した患者の CT の横断面像をトレースし，左右の椎弓根間距離，椎骨動脈間距離，硬膜管横径などを計測する（A)。側面像も同様にトレースし，移植骨長，使用するプレート長，スクリュー長の計画を練る（B)。

必発であることから致命的となり得る。喫煙は神経症状の回復や骨癒合も遅延させる可能性もあり，広範囲前方除圧固定術を適応する場合には最低でも術前 4 週間は絶対的な禁煙とし，守られない場合には手術を延期している。

また，頚椎局所の準備として重要なのは，神経症状の誘発される肢位をあらかじめ把握しておくことである。特に C2 にアプローチする場合には若干伸展気味になるので，意識のある状態で同じ肢位を 10 分間程度とらせ，神経症状が悪化しないことを確認する必要がある。これをしないと，除圧完了前の術中肢位による神経症状悪化を予測できない。同様に，OPLL に対する広範囲前方除圧固定術における術中の脊髄機能モニタリングは，現在のわが国の医療安全に関する環境を考慮すればほぼ必須の検査となりつつある[8]。脊髄機能モニタリング設備がなく，過去に十分な症例経験がない場合には，より専門的な医療機関に紹介することも考慮すべきであろう。

Ⅱ. 手術計画
―除圧固定範囲―

広範囲前方除圧固定術では，上下方向だけでなく，特に OPLL では術前の画像診断により，骨化の成熟度や脊柱管の程度，椎骨動脈の位置に留意しなければならない。側面前後屈 X 線像では骨化の動きに注目する。骨化の切れ目の動きが責任高位であることが少なくない。MRI での脊髄圧迫の程度を参考にしつつ，CT 水平断像および再構成像の正面および側面像で骨化の正確な範囲と形状を把握した上で，paper surgery によって手術計画を立てる（図 2)。MRI で見られる靱帯肥厚部も除圧範囲に含める必要があり，椎体切除部位は脊髄圧迫がない位置に予定する[9]。

広範囲前方除圧固定術は脊髄が同時に広範囲に除圧できるという点で，後方椎弓形成術と同等の効果を持ち得る。骨化浮上術では骨化の前方移動自体に 4～8 週間必要である[10]が，神経組織に対する除圧効果は骨化の切り離しの直後から得られ

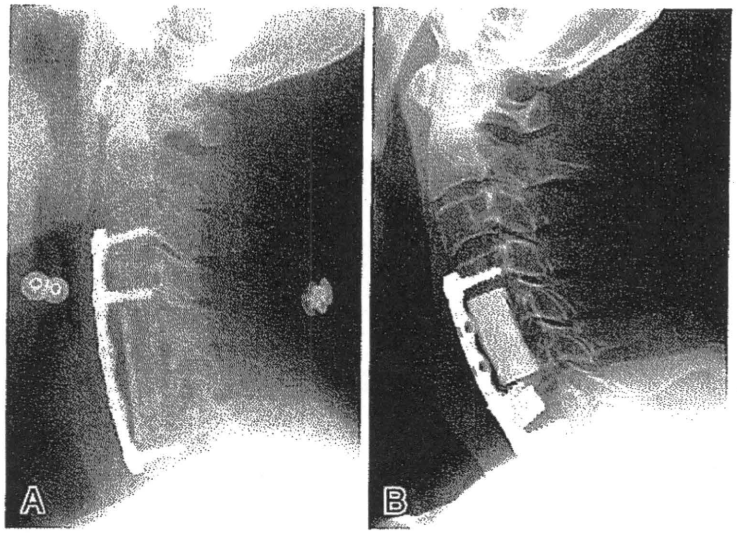

C2-6 固定（腓骨移植）　　C3-7 固定（人工骨移植）

図 3　ハイブリッド固定

上下方向の固定範囲に関しては，OPLL が存在する範囲は連続除圧するものの，アライメント調整や不安定性の予防によって固定範囲に含めざるを得ない隣接椎間に関しては，別に椎間固定のみを追加するようになった。

る。その効果を維持するために安定した脊柱の再建が重要となる。

上下方向の固定範囲に関しては，かつては可及的に広範囲としていたが，現在ではできるだけ分節固定を併用するよう心がけている。除圧操作自体は広範囲である方が容易だが，固定に関して除圧範囲の間に椎体を残すことでスクリューのアンカーポイントを増やすことが可能となり，術直後の固定性は増す。そのため，OPLL が存在する範囲は除圧するものの，アライメントや不安定性によって固定範囲に含めざるを得ない隣接椎間に関しては，別に椎間固定のみを追加するハイブリッド固定を行うようになった（図 3）。

Ⅲ．除圧操作

CSM に対して前方法を選択するときには，多椎間であっても基本的に分節固定を行う。椎間板の廓清ののち，顕微鏡下に後方の骨棘を削る。

OPLL では鉤椎関節を目安に最低でも骨化横径から 1～2 mm の余裕を持たせて，除圧の横径は椎体部で 20 mm，椎間板部では 20 mm 以上を目安にする。その後，椎間板と椎体を交互に切除して，次第に骨溝を深めていく。椎体前面から垂直に掘っていくことが重要であり，掘削が斜めになると術前に計画した除圧横径が確保できないか，骨化が片浮きとなって脊髄の偏在圧迫を起こし Brown-Séquard syndrome を惹起する可能性がある。

Ⅳ．脊柱再建術

1．移　植　骨

1 椎間の分節固定および 1 椎体の椎体亜全摘後の 2 椎間固定には，既成のハイドロキシアパタイトの人工骨を用いている[11)12)]。3 椎間以上の脊柱再建には通常，遊離腓骨移植を行う（図 4）。

椎体母床はできるだけ終板を温存することで，subsidence を防止する。多椎間の椎体亜全摘後の母床作成でも終板のトリミングは行わないが，腓骨の前方部分に作成した peg（くい）を差し込む溝を作成することが多い。

移植骨長は，術野の外から頚椎をわずかに伸張させ，腓骨を軽くたたきこむことで挿入できる程度としている。挿入時に頚椎を伸張しすぎると，脱転の可能性が高まる印象がある（定量的な検討

はなされていない)。

2．プレート固定

腓骨を設置した後に，プレートによる内固定を行う。プレートには，スクリューとの間に動きがないconstrained typeと，上下あるいは回旋の動きをわずかに許容しつつ，抜去される方向には動かないsemi-constrained typeがある。最近ではsemi-constrained typeでの成績が良いという報告が多い[13)~16)]。われわれは使用するスクリューの種類によってconstrained typeにもsemi-constrained typeにも利用できるプレートシステムを主として用いている。スクリューは下位端をfixed type，上位端をvariable typeとしているが，メーカのデータによれば上位で2°程度の回旋が許容される。Semi-constrained typeのプレートには，これ以外にも上下方向のtranslationが数mmにもわたって許容されるタイプもあるが，プレートの種類による臨床成績の差異は明らかになっていない。

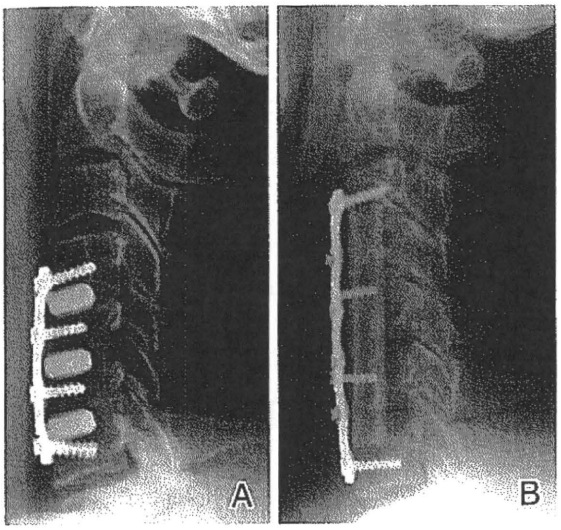

C4-7分節固定　　C3-7椎体亜全摘固定

図4　分節固定と椎体亜全摘固定

1椎間の分節固定および1椎体の椎体亜全摘後の2椎間固定には，既成のハイドロキシアパタイトの人工骨を用いている（A)。3椎間以上の脊柱再建には通常，遊離腓骨移植を行う（B)。

V．合併症（自験例）

過去10年間に行われた3椎間以上の広範囲前方手術のうち，術後1年以上経過観察が可能であった40例（男性36例，女性4例）を対象として，周術期の再建合併症とsubsidenceに関して調査した。手術術式は，椎体亜全摘を行わず椎間ごとに骨移植を行う分節固定（segmental fusion：SF群)，椎体亜全摘除圧固定(long fusion：LF群)，両者の併用（hybrid fusion：HF群）の3群に分類した。SF群は3椎間6例，4椎間1例の計7例，LF群は3椎間14例，4椎間10例，5椎間1例の計25例，HF群は3椎間2例，4椎間4例，5椎間2例の9例であった（表1)。疾患別にはCSM 10例，頚椎症性筋萎縮症3例，後縦靱帯骨化症27例で，頚椎症では7例がSF群，6例がLF群，後縦靱帯骨化症では19例がLF群，8例がHF群であった。後療法は術後2~4日以内に顎つきカラーで起座歩行を開始し，3カ月間外固定を継続した。手術時間は3時間25分~9時間15分（平均5時間53分)，出血量は78 m*l*~2,885 m*l*（平均375 m*l*)，入院期間は15日~79日（平均29日）であった。神経合併症はC5麻痺が2例，脊髄麻痺悪化1例で，うち1例が移植腓骨の移動によるものであった。

表1　対象患者の背景

固定方式	計	3椎間	4椎間	5椎間	移植骨（腓骨：人工骨）
分節固定群（SF）	7	6	1	0	7（1：6）
亜全摘固定群（LF）	25	14	10	1	25（25：0）
ハイブリッド群（HF）	8	2	4	2	8（5：3）
計	40	22	15	3	

SF：分節固定，LF：椎体亜全摘固定，HF：分節固定＋椎体亜全摘固定

1．術後早期の再建合併症

固定に伴う合併症は移植腓骨のC7での転位が2例，C7椎体の母床骨折が2例，スクリュー突出単独が3例で，計7例（17.5%）であった（表2）。再建合併症は，SF群7例にはみられず，HF群2例とLF群5例に起きていた。特に移植骨脱転と母床骨折の4例はいずれも移植骨下端のC7に認めた。また，髄液漏・感染・食道損傷はなかったが，1例では術後長期に嚥下困難が継続した。術後の再手術は神経症状悪化3例と移植骨転位あるいは母床骨折4例の6例（1例にC5麻痺と再建合併症が重複）に行われた。神経症状悪化例に対しては除圧追加を，再建合併症に対しては固定範囲の後方ワイヤリングを行った。スクリュー突出では直後に締め直しが1例，骨癒合後の抜去が2例であった。平均術後3年の最終観察時の移植骨偽関節は4例にみられたが，再建合併症による再手術例ではなかった。後方ワイヤリングが行われた4例ではすべて骨癒合が得られた。この間のJOAスコアの改善率は疾患，偽関節，再建合併症で差はなかった（表3）。

画像計測によれば，再建合併症がみられた群では，頚椎の前弯が強い傾向があり，特に術直後の固定範囲の前弯が有意に強かった。それ以外の危険因子として可能性のある終板の侵襲，移植骨の種別，中間スクリューの使用などに関しては，統計学的に再建合併症の有無とは関連がなかった[17]。

表2 合併症

神経症状の悪化（例数）	
C5麻痺	2
脊髄症悪化	1
再建合併症	
移植骨転位	2*
C7母床骨折	2*
スクリュー突出	3 (5)**

移植腓骨のC7での転位が2例，C7椎体の母床骨折が2例（それぞれ1例ずつにスクリュー突出合併*），スクリュー突出単独が3例で，計7例（17.5%）であった**。

2．移植骨のsubsidence

次に，再建合併症の発生に関して，移植骨の術後早期のsubsidenceの程度をretrospectiveに調査し，スクリューのpulloutへの影響を検討した。対象は40例中，術後早期に移植骨の転位または母床骨折のみられた4例を除いた36例で，術後1カ月の時点で3例にスクリューの突出がみられた。

術後1週間前後の起坐開始直後と1カ月程度経過したのちに撮影された頚椎単純X線中間位側面像において，プレート長を基準として，固定上下端椎体の終板間距離を計測して比較した。その結果，術後約1週間と約1カ月後で，平均1.8%のsubsidenceが認められた。3椎間では1.3±1.3%，4椎間では2.4±1.2%，5椎間では3.0±2.2%であり，絶対値では1～3 mm程度にあたる。術式別にはSF群1.9±0.7%，LF群1.6±1.5%，HF群2.3±1.1%で群間に統計学的に有意差はなかった。使用したスクリューによりconstrained typeのプレートとして機能するはずの5例でも1.5%程度のsubsidenceがみられ，semi-constrained typeのプレート固定と有意差はなかった。また，C7椎体の水平面に対する角度が小さいとsubsidenceが大きい傾向がみられた。

Ⅵ．考　察

—プレート固定の利点と留意点—

広範囲の前方除圧の適応は，疾患と頚椎アライ

表3 術後成績

比　較	JOAスコア改善率
疾患別（CSM 13例：OPLL 27例）	60%：63%
偽関節（骨癒合完成36例：偽関節4例）	62.4%：59.5%
再建合併症（なし33例：あり7例）	62.4%：60.8%

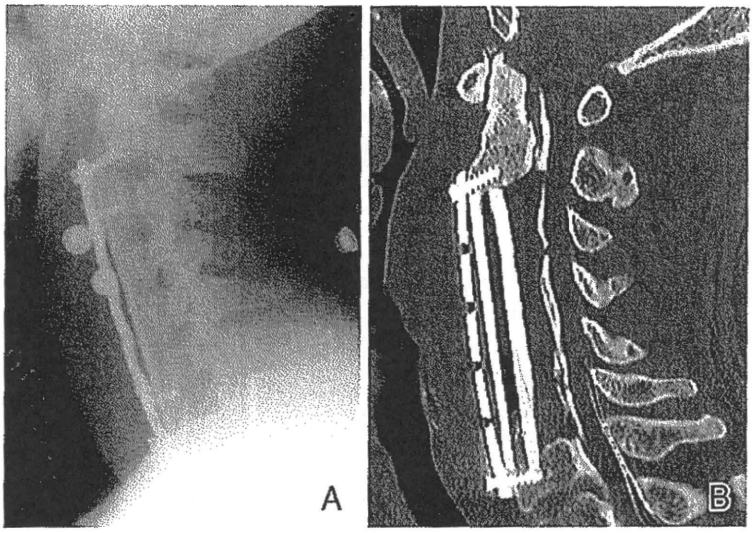

術後7日の単純X線側面像　　同日のCT再構成側面像

図5　CT再構成側面画像による再建合併症の評価
術直後にルーチンで撮影されるポータブルX線像では，移植骨の転位やスクリューの突出は正確に把握できないことが多いが（A），CTの再構成像でC7スクリューの突出も明瞭にわかる（B）。

メント，脊髄に対する圧迫様式により決定され，後方除圧よりも前方から除圧を試みた方がよい症例が一定程度存在する。その後の再建に関して，従来はハローベストによる固定が行われたが，現在の医療環境からすれば，6〜8週間にも及ぶハローベスト装着は困難になりつつある。また，術直後の呼吸不全への対応も外固定がない方が容易であることは自明であろう。さらに，頚椎の固定で，術後成績が安定する可能性もある。われわれの経験では，前方固定と後方除圧（非固定）を比較したところ，CSMでもOPLLでも術後4〜5年で前方法の方が安定した術後成績を保っていた[18)19)]。

一方，前方法では固定隣接椎間板の変性加速が長期の合併症として知られている。しかし，広範囲前方除圧固定術では，あらかじめ相対的な狭窄や不安定性がある隣接椎間を固定範囲に含めていたためか，今回のシリーズでは神経症状再発はみられなかった。河村ら[20)]の4椎間以上の前方除圧固定術において固定隣接椎間障害発生がそれ以下よりも少なかったという報告に合致する。しかし，松岡ら[21)]によれば，術後平均13年のOPLLに対する頚椎広範囲前方除圧固定術（プレート非使用）57例の長期成績では，隣接椎間障害は6例に認められ再手術が行われたとされる。今後，経過年数が長くなるとC6/7やC7/T1など下位椎間障害が問題となるかもしれない。

自験例からは，プレートを使用しても早期再建合併症は一定頻度で発生し得ることがわかった。移植骨の転位や母床の骨折などの再建合併症は術後1週間以内に開始される起坐より以前，あるいはその直後に発見されていた。固定下位端に起きるために，術直後にルーチンで撮影されるポータブルX線像では，移植骨の転位やスクリューの突出は正確に把握できないことが多いが，CTの再構成像で明瞭となる（図5）。本シリーズでは再建合併症に対して安静臥床の長期化やハローベストによる外固定追加は行わなかったが，移植骨の転位が進行性の場合に棘突起ワイヤリングを追加した（図6）。その結果，移植骨が完全に脱転した例はなかった。また，1例には突出したスクリューの締め直しを行ったが，いずれも術後1カ月以内に最初の処置が行われた。画像による検討では，再建合併症群で頚椎の前弯が大きい例が多く，移

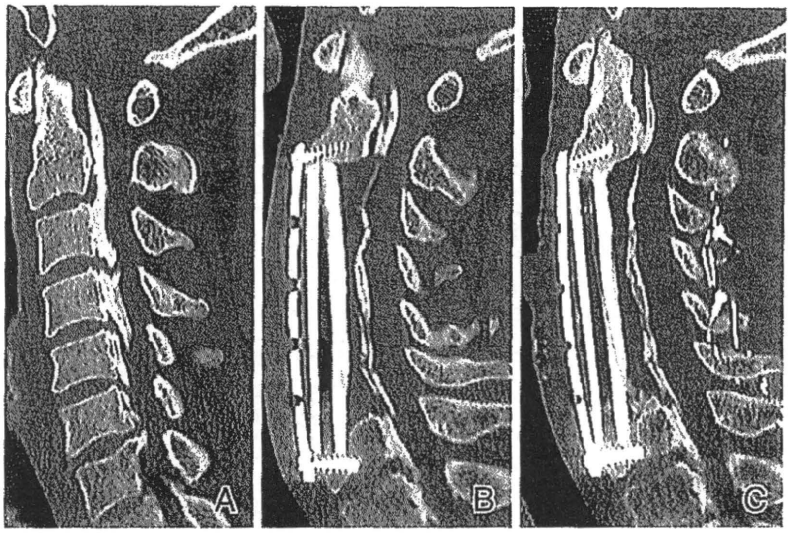

術 前　　術後4週　　術後6カ月

図 6　Salvage 手術としての棘突起ワイヤリング

図5と同一症例で，51歳の OPLL に対して C2-7 前方除圧固定術を行った（A)。術後4週で移植腓骨の明らかな subsidence とともに C7 母床の骨折がみられた（B)。棘突起ワイヤリングを追加し，術後6カ月で骨癒合を得た（C)。

植下位端において発生する剪断力が再建合併症の発生に影響している可能性が示唆された。一般に脊髄の除圧には頚椎の前弯が望ましいと考えられているが，広範囲前方除圧固定術においては過度の前弯にならないようにすべきであろう。

一方，術後早期に移植骨転位や母床骨折がみられなかった36例では，移植骨の subsidence は1〜3 mm 程度みられたのみで，その後のスクリューの突出とは関連性がみられなかった。Hughes ら[22] は，プレートを用いない2〜3椎体の亜全摘後の腓骨移植で，術後2年で6.7±5.7 mm の subsidence が起きていたことを報告した。本シリーズではそこまでの subsidence は発生していなかったが，constrained type を使用しても subsidence は生じており，細江ら[23] の術後1年で4 mm 程度の短縮を認めたとしている報告と同様であった。広範囲前方除圧固定術では，一定程度の subsidence は不可避と考えられる。終板切除により subsidence がより大きくなることが予想されるが，本シリーズでは明らかな影響は見いだせなかった。

おわりに

以上のように，広範囲頚椎前方除圧固定術は，前方プレートにより術後管理が容易となり，安静臥床やハローベストによる外固定も不要になった。しかし，再建合併症が一定頻度でみられ，特に頚椎の前弯が強いケースで固定下位端での移植骨トラブルが目立った。移植骨が完全に脱転する前に棘突起ワイヤリングを追加することで対処は可能であったが，ケースによっては最初から前後同時固定を考慮するなどの対処が必要もかもしれない[24][25]。

文　献

1) Iwasaki M et al：Surgical strategy for cervical myelopathy due to ossification of the posterior longitudinal ligament. Spine **32**：654—660, 2007
2) Masaki Y et al：An analysis of factors causing poor surgical outcome in patients with cervical myelopathy due to ossification of the posterior longitudinal ligament；anterior decompression with spinal fusion versus laminoplasty. J Spinal Disord Tech **20**：7—13, 2007
3) Suda K et al：Local kyphosis reduces surgical

outcomes of expansive open-door laminoplasty for cervical spondylotic myelopathy. Spine **28**：1258−1262, 2003
Hilibrand AS et al：Increased rate of arthrodesis with strut grafting after multilevel anterior cervical plating. Spine **27**：146−151, 2002
5) 池永　稔ほか：自家腓骨を用いた4椎間以上頚椎前方固定術の成績. 中部整災誌 **46**：449−450, 2003
6) Sasso RC et al：Early reconstruction failures after multilevel cervical corpectomy. Spine **28**：140−142, 2003
7) Daubs MD：Early failures following cervical corpectomy reconstruction with titanium mesh cages and anterior plating. Spine **30**：1402−1406, 2005
8) Shinomiya K et al：Anterior cervical decompression for cervical myelopathy caused by ossification of the posterior longitudinal ligament (OPLL). OPLL；Ossification of the Posterior Longitudinal Ligament, 2nd ed, Springer, 209−218, 2006
9) 進藤重雄ほか：多椎間連続型巨大頚椎後縦靱帯骨化症に対する前方除圧固定術（浮上術）. 執刀医のためのサージカルテクニック−脊椎アドバンス，メジカルビュー，46−65，2008
10) Yamaura I et al：Anterior floating method for cervical myelopathy caused by ossification of the posterior longitudinal ligament. Clin Orthop **356**：27−34, 1999
11) 末綱　太：前方プレート. 関節外科 **27**：96−105, 2008
12) 新井嘉容ほか：人工骨-骨髄ハイブリッド移植による頚椎前方固定術. OS Now No. 6：20−33, 2008
13) Dipaola CP et al：Screw orientation and plate type (variable- vs fixed-angle) effect strength of fixation for in vitro biomechanical testing of the Synthes CSLP. Spine J **8**：717−722, 2008
14) Nunley PD et al：Choice of plate may affect outcomes for single versus multilevel ACDF；results of a prospective randomized single-blind trial. Spine J **9**：121−127, 2009
15) Stulik J et al：Fusion and failure following anterior cervical plating with dynamic or rigid plates；6-months results of a multi-centric, prospective, randomized, controlled study. Eur Spine J **16**：1689−1694, 2007
16) Pitzen TR et al：Implant complications, fusion, loss of lordosis, and outcome after anterior cervical plating with dynamic or rigid plates；two-year results of a multi-centric, randomized, controlled study. Spine **34**：641−646, 2009
17) Okawa A et al：Hyperlordosis of the cervical spine is a risk factor for reconstruction failure of 3-level or greater anterior cervical decompression and anterior plate fixation fusion. JSSR **20**：761−765, 2009
18) 坂井顕一郎ほか：頚椎後縦靱帯骨化症の中期手術成績−前方手術と後方手術の前向き比較研究. 日整会誌 **83**：S78, 2009
19) Hirai T et al：Clinical outcome of surgical treatment for cervical spondylotic myelopathy；a prospective comparative study between anterior decompression and fusion (ADF) and posterior decompression with laminoplasty-5-year follow-up. Presented in the 37th Annual Meeting of the Cervical Research Society, 2009
20) 河村真吾ほか：頚椎多椎間（4椎間以上）前方除圧固定術において固定隣接椎間障害発生が問題となるか？　日脊会誌 **20**：508, 2009
21) 松岡　正ほか：頚椎後縦靱帯骨化症に対する骨化浮上術の長期成績. 別冊整形外科 No. 45：155−161, 2004
22) Hughes SS et al：Settling of fibula strut graft following multilevel anterior cervical corpectomy. Spine **31**：1911−1915, 2006
23) 細江英夫ほか：頚椎亜全摘前方固定術後の腓骨定着と内固定材料の変化. 脊椎・脊髄神経手術手技 **10**：117−119, 2008
24) Gok B et al：Surgical treatment of cervical spondylotic myelopathy with anterior compression；a review of 67 cases. J Neurosurg Spine **9**：152−157, 2008
25) Dogan S et al：Biomechanical consequences of cervical spondylectomy versus corpectomy. Neurosurgery **63**(Suppl 2)：303−308, 2008

Effects of Gamma-Ray Irradiation on Mechanical Properties, Osteoconductivity, and Absorption of Porous Hydroxyapatite/Collagen

Yuichi Kawasaki,[1] Shinichi Sotome,[1,2] Toshitaka Yoshii,[1] Ichiro Torigoe,[1] Hidetsugu Maehara,[1] Yumi Sugata,[1,3] Masahiro Hirano,[4] Naomi Mochizuki,[4] Kenichi Shinomiya,[1,3,5,6] Atsushi Okawa[1]

[1] Department of Orthopaedic and Spinal Surgery, Graduate School, Tokyo Medical and Dental University, Bunkyo-ku, Tokyo 113-8519, Japan

[2] Department of Regenerative Therapeutics for Spine and Spinal Cord, Graduate School, Tokyo Medical and Dental University, Bunkyo-ku, Tokyo 113-8519, Japan

[3] Global Center of Excellence (GCOE) Program, International Research Center for Molecular Science in Tooth and Bone Disease, Tokyo Medical and Dental University, Bunkyo-ku, Tokyo 113-8519, Japan

[4] PENTAX New Ceramics Division, HOYA Corporation, Itabashi-ku, Tokyo 174-8639, Japan

[5] Hard Tissue Genome Research Center, Tokyo Medical and Dental University, Chiyoda-ku, Tokyo 101-0062, Japan

[6] Core to Core Program for Advanced Bone and Joint Science, Tokyo Medical and Dental University, Chiyoda-ku, Tokyo 101-0062, Japan

Received 28 February 2009; revised 28 June 2009; accepted 16 July 2009
Published online 2 October 2009 in Wiley InterScience (www.interscience.wiley.com). DOI: 10.1002/jbm.b.31502

Abstract: In this study, the effects of gamma-ray irradiation on the mechanical properties, absorbability, and osteoconductivity of porous hydroxyapatite/collagen (HAp/Col) were investigated. Porous HAp/Col was exposed to 16, 25, 35, or 50 kGy of gamma-ray irradiation. The compressive elastic modulus showed irradiation dose-dependence, with a particularly pronounced decrease in the 50-kGy treatment group. An *in vitro* enzymatic digestion test showed that gamma-ray irradiation of porous HAp/Col resulted in accelerated degradation by collagenase. For *in vivo* studies, porous HAp/Col was transplanted into the back muscles or bone defects in the femoral condyle of rats. Specimens were obtained at 2, 4, and 8 weeks postoperatively. Absorption of the implants in the muscle was time- and irradiation dose-dependent, with notable absorption for the 35- and 50-kGy groups at 2 weeks. At the skeletal sites, porous HAp/Col demonstrated high osteoconductivity in all irradiation treatment groups. Interestingly, not only implant absorption but also bone formation was irradiation dose-dependent at early time points. © 2009 Wiley Periodicals, Inc. J Biomed Mater Res Part B: Appl Biomater 92B: 161–167, 2010

Keywords: gamma ray irradiation; osteoconduction; bioabsorption; hydroxyapatite composite; collagen

INTRODUCTION

Artificial bone substitutes are widely used to reconstruct bone defects caused by tumors, trauma, and other adverse events. Sintered calcium phosphates and their composites have been the materials most widely used as bone substitutes,[1–4] although a variety of composites composed of inorganic and organic materials such as hydroxyapatite/collagen (HAp/Col) have also been developed recently.

HAp/Col has a nanostructure similar to that of natural bone; it is composed of nanoscale needle-like HAp crystals with *c*-axes aligned along type I atelocollagen fibers derived from porcine skin. The HAp/Col weight ratio is 80:20.[5] Previous reports using HAp/Col implants with different macrostructures (dense or porous HAp/Col or as a composite with alginate) have demonstrated satisfactory osteoconductivity and bioabsorption when the implants were used as a bone substitute.[6–9] Above all, porous HAp/Col is a promising bone substitute for clinical use

Correspondence to: S. Sotome (e-mail: sotome.orth@tmd.ac.jp)
Contract grant sponsor: The Ministry of Education, Culture, Sports, Science and Technology of Japan

because it has a sponge-like elasticity that makes it easy to handle during surgery. It can also be used as a drug delivery carrier for bone reconstruction.[9]

For clinical implementation of HAp/Col, sterilization is necessary. However, available sterilization methods are limited because of the distinctive composition of this material. Ethylene oxide gas, one of the most popular means of sterilization, stably adsorbs onto HAp crystals because of their broad adsorptive area.[10] Autoclaving also cannot be used for HAp/Col sterilization because the high-pressure steam severely disrupts the collagen fibers while leaving HAp crystals intact.[11,12] Therefore, these common sterilization methods are inappropriate for preparing HAp/Col for clinic use.

Although gamma-ray irradiation also disrupts collagen fibers to some degree, the severity of this disruption is much lower than that caused by autoclaving.[13] However, the specific effects of gamma rays on collagen fibers or collagen-containing composites have not been established. A previous study reported that 25 kGy of gamma-ray irradiation affected not only resistance to enzymatic digestion and the porous structure of a collagen sponge but also *in vitro* cell migration into the sponge.[14] Another group reported that 15-kGy irradiation of a bone graft did not compromise its efficacy.[15] There are many other conflicting reports about the effects of gamma rays on collagen or collagen-based composites.

In this study, the effects of a variety of doses of gamma-ray irradiation on the mechanical properties, bioabsorbability, and osteoconductivity of porous HAp/Col were examined.

MATERIALS AND METHODS

Preparation of Porous Hydroxyapatite/Collagen

HAp/Col nanocomposite fibers were synthesized from a $Ca(OH)_2$ suspension and H_3PO_4 solution, which contained atelocollagen derived from porcine skin, using a previously reported coprecipitation method.[5] Briefly, 400 m*M* $Ca(OH)_2$ and 120 m*M* H_3PO_4 containing dissolved collagen (atelo-type I collagen from porcine dermis; Nitta Gelatin, Japan) were simultaneously added slowly to distilled water kept at 40°C in a water bath. The speed of the dropwise addition was controlled to maintain the pH at 9.0. The initial HAp/Col weight ratio was 80:20. The obtained HAp/Col precipitate was lyophilized and used to prepare porous HAp/Col. Next, 1 g of HAp/Col fibers was homogenized with 6.5 mL of phosphate-buffered saline (PBS) and alkalized with 50 μL of 1*M* sodium hydroxide solution. This mixture was combined with 1.5 mL of 0.6% collagen in phosphoric acid (pH 2.0). The resultant mixture (pH 7.0) was infused into a mold. To initiate gelation of collagen as a binder, the mold containing the mixture was incubated at 37°C for 2 h. Next, the gelled mixture was frozen at −60°C, allowing the remaining liquid to form ice crystals within the gel. The spaces occupied by the ice crystals were converted to pores by subsequent lyophilization. These lyophilized porous HAp/Col composites were dehydrothermally treated at 140°C for 12 h in a vacuum to introduce crosslinking of the collagen molecules. Porous HAp/Col was then cut to samples 10 mm × 10 mm × 10 mm in size for mechanical testing, 10 mm × 10 mm × 5 mm for *in vitro* bioabsorption testing, and 2 mm × 2 mm × 3 mm for *in vivo* analyses. The porous HAp/Col constructs were sterilized by gamma-ray irradiation at 16, 25, 35, or 50 kGy or treated with 70% ethanol for 10 min as a control.

Mechanical Testing

The compressive mechanical properties of porous HAp/Col with a 10 mm × 10 mm × 10 mm cubic shape were analyzed using a mechanical examination machine with a load cell capacity of 20 N, (N = 5) (EZ test-20N; Shimadzu Corporation, Japan). The specimens were moisturized by soaking in distilled water for 2 min under vacuum to remove the remaining air in the pores, causing them to become elastic and sponge-like. Each specimen was compressed perpendicularly at a cross-head speed of 10 mm/min to achieve a strain of 25% and then was immediately returned to the initial position. This cyclic test was repeated four times. The recovery rate and the compressive elastic modulus at 10 and 20% strain were calculated from the stress–strain curve of the fourth compression. After the compression test, the specimens were prepared for observation by scanning electron microscopy (SEM).

SEM Examination

After mechanical compressive testing, the specimens were fixed with 2.5% glutaraldehyde, cut at the center, and post-fixed with 0.1% osmium tetroxide. Next, the samples were dehydrated through a graded series of ethanol washes, dried by a critical point dryer, mounted onto aluminum stubs, and sputter-coated with platinum. The samples were observed from the cut plane using a SEM (Hitachi S4200 FESEM, HITACHI, Tokyo, Japan).

In Vitro Bioabsorption

The *in vitro* bioresorbability of porous HAp/Col was tested using the collagenase digestion model reported by Yunoki et al.[16] Blocks of porous HAp/Col (10 mm × 10 mm × 5 mm) with a weight of 70.3 ± 3.0 mg (mean ± SD) were immersed in 5 mL PBS containing 375 U of bacterial collagenase (*Clostridium histolyticum*; Wako Pure Chemical Industries) and incubated at 37°C for 1 (N = 3) or 2 (N = 6) h. The collagenase solution and the sediment of degraded HAp/Col were then removed using a pipette. The remaining HAp/Col blocks were frozen, freeze-dried, and weighed. The remaining weight was normalized against the initial weight by taking the percentage.

Surgical Procedures

All experimental animals used in these studies were maintained and treated according to the guidelines for the care and use of laboratory animals of the Tokyo Medical and Dental University. After anesthesia by intraperitoneal administration of 7% trichloroacetaldehyde monohydrate solution (0.5 mL per 100 g of body weight) and aseptic preparation, HAp/Col implants were transplanted into bone defects created in the distal ends of the femurs and into pouches in the back muscles of male rats (F344, age 11 weeks, weight 240–250 g). The distal end of the femur shaft was exposed by lateral approach and a 3-mm diameter hole was bored using an electric drill with continuous saline irrigation. The drill hole was then rinsed with saline, and the implant was placed in the hole. At 2, 4, and 8 weeks post-transplantation, the rats were euthanized and the femurs and composites transplanted into the back muscles were excised.

Quantification of Porous HAp/Col in Back Muscle

Porous HAp/Col implants removed from the dorsal muscle were scanned using a micro-CT scanner (ScanXmate-E090; Comscantecno, Japan) before fixation to exclude the effects of fixation on sample volume. Three-dimensional image data were then reconstructed, and the volume of the porous implant was calculated using the three-dimensional bone analysis software TRI/3D-BON (Ratoc System Engineering, Japan).

Histological Analysis

After micro-CT analysis, samples were fixed in 4% paraformaldehyde, decalcified in 20% ethylenediaminetetraacetic acid (EDTA), dehydrated using a graded alcohol series, and embedded in paraffin wax. Sections of 5-μm thickness were cut and stained with hematoxylin and eosin (HE) or tartrate-resistant acid phosphatase stain (TRAP).

Statistical Analysis

Overall differences among groups in the mechanical test were determined by two-factor repeated measures analysis of variance (ANOVA), and those in the other experiments were determined by two-factor ANOVA, and differences between individual groups were estimated using the Tukey-Kramer multiple comparison test. Differences were considered statistically significant when the p value was <0.05.

RESULTS

Compressive Mechanical Test

Swelling of the samples after rehydration was not detected by macroscopic observation. All tested samples behaved elastically, and recovery rates after the fourth compression were greater than 92% in all groups, although there was a slight irradiation dose-dependent decrease in recovery rate (Table I). Compared to the nonirradiated control, the compressive elastic modulus of all irradiated groups was markedly decreased at strains of both 10 and 20%, with the lowest modulus observed in the 50-kGy group [Figure 1(A)]. SEM images of porous HAp/Col specimens after mechanical testing demonstrated that although slight compressive deformation of the porous structures remained, there was no apparent disruption of the materials in any group, including those treated with 50-kGy irradiation [Figure 1(B)].

TABLE I. Recovery Rates of Compression Test

Control	16 kGy	25 kGy	35 kGy	50 kGy
94.3%	93.4%	93.5%	93.1%	92.8%

In Vitro Bioresorbability

Figure 2 shows the remaining weight of the HAp/Col composite after enzymatic digestion by collagenase. As the irradiation dose increased, the remaining weight decreased. The reduction ratios of the remaining porous HAp/Col in the 35- and 50-kGy groups were significantly higher than those of the other groups.

Quantification of Porous HAp/Col in Back Muscle

Figure 3 shows the volume of residual porous HAp/Col extracted from the back muscle. Control implants were scarcely absorbed until 8 weeks after transplantation. In contrast, all irradiated implants showed dose-dependent decrease in volume, with the 35- and 50-kGy irradiation-treated specimens exhibiting drastic volume decreases 2 weeks postoperatively. The average volume of the 50-kGy group was increased slightly at 4 and 8 weeks, where this may have been due to dispersion of the fragmented implant following tissue invasion.

Histological Analysis

Porous HAp/Col at the Extraskeletal Site. Fragmentation of porous HAp/Col implants and multinucleated macrophage attachment were observed in all irradiated groups at 2 weeks post-transplantation. The 50-kGy-treated implants were the most severely fragmented and reduced, with a large number of multinucleated macrophages attaching to the fragments. In the control group, despite the presence of macrophages, the porous structure of the extracted implants was maintained (Figure 4).

At 4 weeks after implantation, although the extracted implants in the 16-, 25-, and 35-kGy groups were almost completely fragmented and the original porous structures could not be recognized, the volume of the remnants of the 35- and the 50-kGy implants was still lower. Partial fragmentation of the control implant was also observed at 4 weeks postoperatively. At 8 weeks, absorption of the 25-

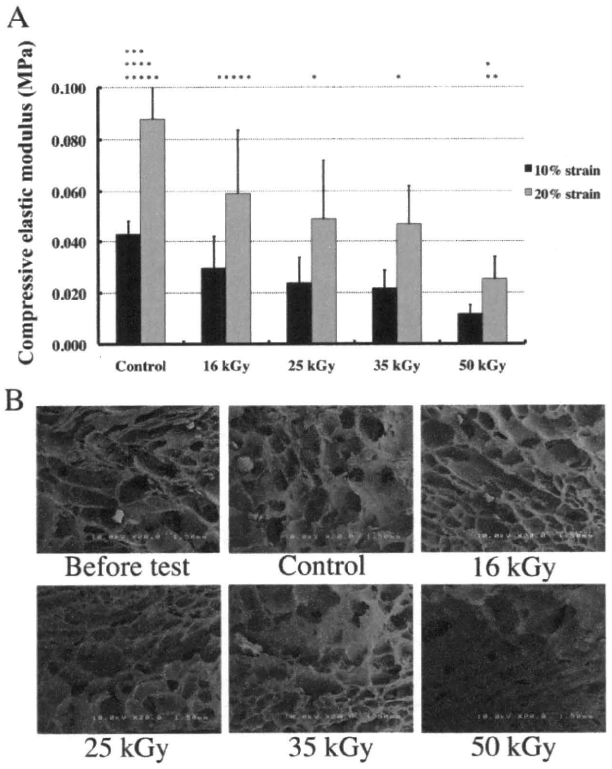

Figure 1. (A) Elastic moduli of porous HAp/Col after gamma-ray irradiation at 10 and 20% strain ($N = 5$). *$p < 0.05$ versus control, **$p < 0.05$ versus 16 kGy, ***$p < 0.05$ versus 25 kGy, ****$p < 0.05$ versus 35 kGy, *****$p < 0.05$ versus 50 kGy. (B) SEM images of the porous structure of HAp/Col before and after compression testing.

kGy implant was advanced when compared with the 16-kGy and control groups. Some control implants even maintained their original porous structure at 8 weeks.

Porous HAp/Col at the Skeletal Site. At 2 weeks after implantation, absorption of the irradiated implants was

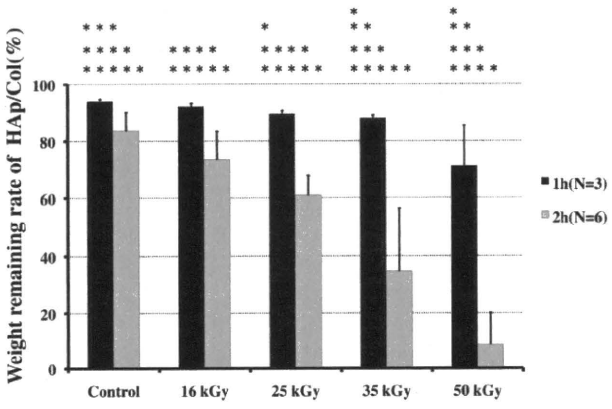

Figure 2. Weight of porous HAp/Col remaining after collagenase digestion. Incubation time of 1 ($N = 3$) or 2 h ($N = 6$). *$p < 0.05$ versus control, **$p < 0.05$ versus 16 kGy, ***$p < 0.05$ versus 25 kGy, ****$p < 0.05$ versus 35 kGy, *****$p < 0.05$ versus 50 kGy.

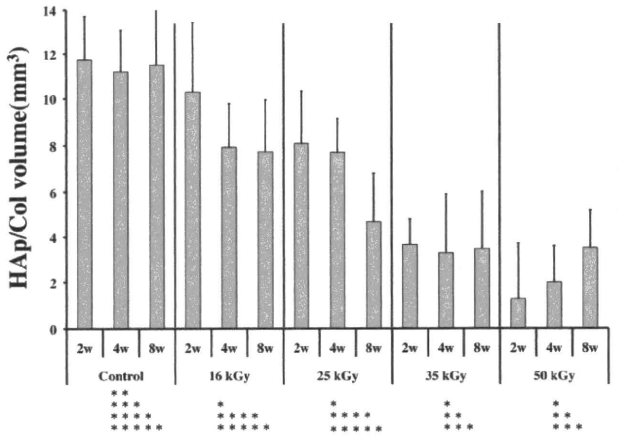

Figure 3. Residual volume of porous HAp/Col in back muscle quantified by micro-CT analysis. *$p < 0.05$ versus control, **$p < 0.05$ versus 16 kGy, ***$p < 0.05$ versus 25 kGy, ****$p < 0.05$ versus 35 kGy, *****$p < 0.05$ versus 50 kGy.

dose-dependent, with bioabsorption, fragmentation, and soft tissue invasion from the extraskeletal site observed for 50-kGy implants. Bone formation in the marrow cavity also showed irradiation dose-dependent increases (Figure 5).

At 4 weeks postoperatively, the bone defects of each group were almost completely closed, with no significant differences in the amount of residual implant or bone tissue in the marrow cavity. At 8 weeks, normal bone marrow cavities were restored; implants and surplus bone in the cavities were almost completely absorbed, and small remnants of the implants surrounded by the bone tissue were observed in all groups.

In 2-week implants, TRAP-positive multinucleated cells were attached to both the cavity and extraskeletal sides, and the number of TRAP-positive cells increased as the irradiation dose increased (Figure 6).

The 4-week implants also exhibited a large number of TRAP-positive cells in every group. The cells were mainly attached to newly formed bone in the 50-kGy gamma-irradiated implants, whereas in the control group, cells mainly adhered to the implant remnant. The number of TRAP-positive cells was markedly decreased at 8 weeks when compared with 2 and 4 weeks postimplantation.

DISCUSSION

In this study, gamma-ray irradiation resulted in dose-dependent reduction of elastic modulus and resistance to biological digestion for porous HAp/Col, although bone conductivity at skeletal implantation sites was not impaired.

Gamma-ray irradiation from Cobalt 60 sources is a popular sterilization method for medical devices, including implant materials. However, gamma-ray irradiation has also been reported to degrade collagen by splitting the peptide chains, thus adversely affecting the mechanical and biological properties of collagen-containing materials.[13,17] Porous

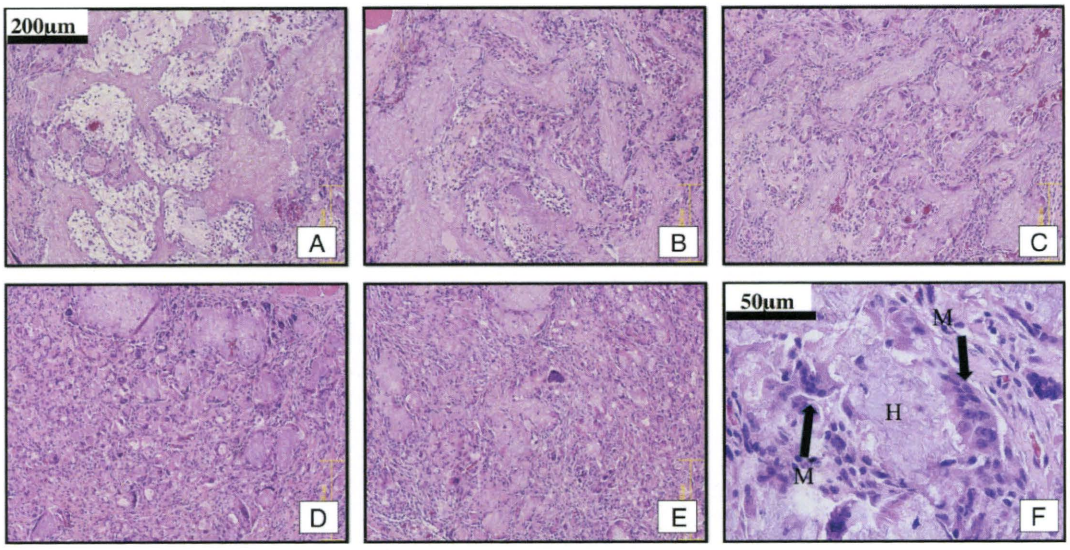

Figure 4. Sections of the HAp/Col implant harvested from back muscle at 2 weeks after implantation (HE staining). (A) Control group (70% ethanol), (B) 16-kGy-irradiated group, (C) 25-kGy-irradiated group, (D) 35-kGy-irradiated group, (E) 50-kGy-irradiated group, (F) high-magnification views of 25-kGy-irradiated group. H, HAp/Col. M, multinucleated macrophage. Implant fragmentation in the 35- and 50-kGy groups was severe. [Color figure can be viewed in the online issue, which is available at www.interscience.wiley.com.]

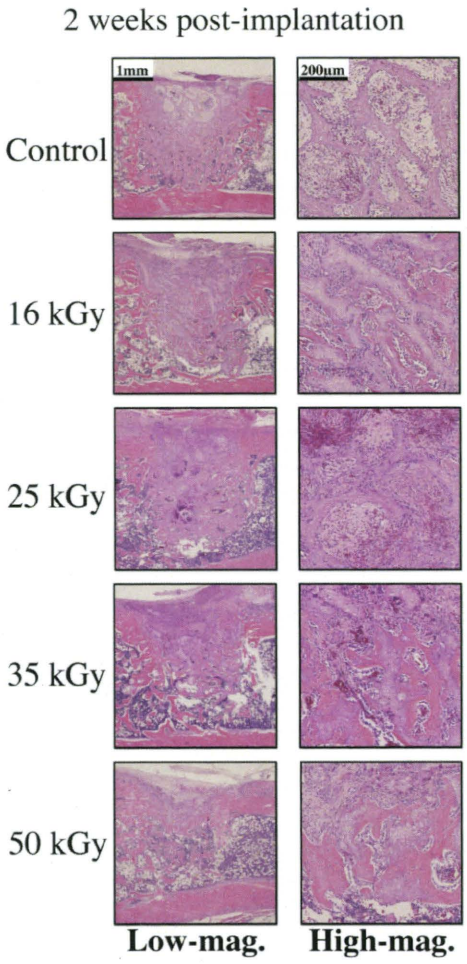

HAp/Col is a bioabsorbable bone substitute with high osteoconductivity and unique mechanical properties including elasticity; these properties permit facile handling during surgery.[9,18,19] Thus, the fragmentation of collagen fibers in HAp/Col by gamma-ray irradiation may significantly affect the ease of use of porous HAp/Col implants.

Porous HAp/Col is elastic and sponge-like and does not have weight-bearing mechanical strength. As a result, its mechanical properties do not contribute directly to its clinical usefulness and, for orthopedic applications, fixation devices must also be used at weight-bearing sites. However, the elasticity of HAp/Col is important for ease of handling and implantation, and therefore, we evaluated the effects of gamma-ray irradiation on elasticity. The elastic moduli of all HAp/Col implants showed irradiation dose-dependent decrease, with the most noticeable decrease observed for the 50-kGy group. Additionally, the 50-kGy-irradiated implants were noticeably fragile during *in vivo* transplantation experiments, although SEM images and the recovery rate after uniaxial compression did not reveal much degradation.

Bone prosthetic materials are commonly used to fill bone defects and accelerate natural bone ingrowth. Ideally, these materials should be absorbed and completely replaced

Figure 5. Coronal sections of femurs crossing the center of the implant 2 weeks postoperatively (HE staining). Left column shows lower magnification (×1.25), right column shows higher magnification (×10). [Color figure can be viewed in the online issue, which is available at www.interscience.wiley.com.]

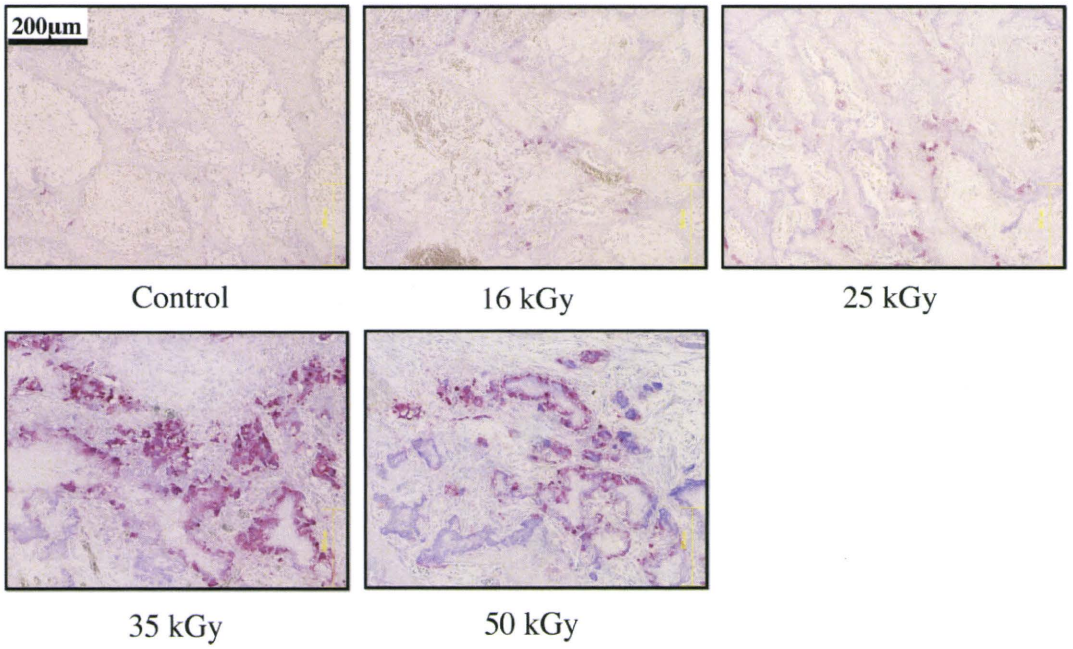

Figure 6. TRAP staining of femur sections 2 weeks postoperatively. The number of TRAP-positive cells was irradiation dose-dependent. [Color figure can be viewed in the online issue, which is available at www.interscience.wiley.com.]

by natural bone in the long term. However, in the clinic, bone defects are not always surrounded by cortical bone or periosteum, and healing may be disrupted by soft tissue invasion of the defect.[20] Bone substitutes implanted in bone defects promote healing by accelerating bone ingrowth due to osteoconductivity and prevention of soft tissue invasion.[21,22] Hence, bone substitutes should resist bioabsorption by macrophages with subsequent soft tissue invasion. Therefore, the effects of gamma-ray irradiation on the bioabsorbability of porous HAp/Col were tested using *in vitro* enzymatic digestion test and *in vivo* implantation models.

In vitro tests were performed using collagenase, which is responsible for collagen degradation *in vivo*.[16] *In vitro* digestion of the HAp/Col implant by collagenase was irradiation dose-dependent, with particularly notable degradation after gamma-ray irradiation at 35 or 50 kGy.

In muscular tissue, the porous HAp/Col nonirradiated implant maintained its volume and porous structure until 8 weeks after implantation, whereas in skeletal implantation sites, implants were almost completely absorbed and replaced by bone tissue. Control implants resisted bioabsorption from the extraskeletal site and soft tissue invasion. Intramuscular absorption of irradiated HAp/Col progressed faster than that of the control, especially for 35-and 50-kGy implants, whose volume decreased markedly at early time points. Absorption of the irradiated implants in the marrow cavities also progressed faster than that of the control, although this absorption was followed by the ingrowth of new bone. Notably, implant absorption and bone ingrowth were synchronized; thus, bone ingrowth of the 50-kGy group was most vigorous at early time points after transplantation. These findings indicate that osteoclast–osteoblast coupling mechanisms might be involved in the osteoconductivity of porous HAp/Col. Although all bone defects treated with irradiated implants eventually healed in the *in vivo* model, concavity and soft tissue invasion were observed on the extraskeletal side of 50-kGy implants due to macrophage adhesion. Thus, if the bone defects had been larger and a porous HAp/Col implant sterilized with 50 kGy or more gamma-ray irradiation had been transplanted, the implant may have been absorbed and the defect may not have healed completely.

In this study, porous HAp/Col was treated with gamma-ray irradiation at 16, 25, 35, and 50 kGy. Irradiation of porous HAp/Col at 16 kGy is the minimum dose for which we could validate sterility (ISO11137-2006, data not shown). Gamma-ray irradiation of porous HAp/Col has few beneficial effects and should thus be applied sparingly. Our results suggest that the proper gamma-ray irradiation dose for sterilization of porous HAp/Col is 16 or 25 kGy.

Porous HAp/Col was jointly developed by the Tokyo Medical and Dental University, the HOYA Corporation, and the National Institute for Materials Science (NIMS). The authors thank Dr. Masanori Kikuchi at NIMS for excellent technical support and advice.

REFERENCES

1. Perry CR. Bone repair techniques, bone graft, and bone graft substitutes. Clin Orthop Relat Res 1999;360:71–86.
2. Giannoudis PV, Dinopoulos H, Tsiridis E. Bone substitutes: An update. Injury 2005;36 (Suppl 3): S20–S27.
3. Finkemeier CG. Bone-grafting and bone-graft substitutes. J Bone Joint Surg Am 2002;84:454–464.
4. Reynolds MA, Aichelmann-Reidy ME, Branch-Mays GL, Gunsolley JC. The efficacy of bone replacement grafts in the treatment of periodontal osseous defects. A systematic review. Ann Periodontol 2003;8:227–265;Review.
5. Kikuchi M, Itoh S, Ichinose S, Shinomiya K, Tanaka J. Self-organization mechanism in a bone-like hydroxyapatite/collagen nanocomposite synthesized in vitro and its biological reaction in vivo. Biomaterials 2001;22:1705–1711.
6. Itoh S, Kikuchi M, Takakuda K, Koyama Y, Matsumoto H, Ichinose S, Tanaka J, Kawauchi T, Shinomiya K. The biocompatibility and osteoconductive activity of a novel hydroxyapatite/collagen composite biomaterial, and its function as a carrier of rhBMP-2. J Biomed Mater Res 2001;54:445–453.
7. Itoh S, Kikuchi M, Koyama Y, Takakuda K, Shinomiya K, Tanaka J. Development of an artificial vertebral body using a novel biomaterial, hydroxyapatite/collagen composite. Biomaterials 2002;23:3919–3926.
8. Sotome S, Uemura T, Kikuchi M, Chen J, Itoh S, Tanaka J, Tateishi T, Shinomiya K. Synthesis and in vivo evaluation of a novel hydroxyapatite/collagen–alginate as a bone filler and a drug delivery carrier of bone morphogenetic protein. Mater Sci Eng C 2004;24:341–347.
9. Sotome S, Orii H, Kikuchi M, Ikoma T, Ishida A, Tanaka J, Shinomiya K. In vivo evaluation of porous hydroxyapatite/collagen composite as a carrier of OP-1 in a rabbit PLF model. Key Eng Mater 2005;309–311:977–980.
10. Sotome S, Uemura T, Kikuchi M, Itoh S, Takakuda K, Tanaka J, Tateishi T, Shinomiya K. In vitro evaluation of highly absorptive ceramics materials needs consideration of calcium and magnesium ions adsorbed to the materials. Key Eng Mater 2002;218–220:153–156.
11. Xiaodu W, Ruud AB, Johan MT, Mauli A. The role of collagen in determining bone mechanical properties. J Orthop Res 2001:19:1021–1026.
12. Draenert GF, Delius M. The mechanically stable steam sterilization of bone grafts. Biomaterials 2007;28:1531–1538.
13. Nguyen H, Morgan DA, Forwood MR. Sterilization of allograft bone: Effects of gamma irradiation on allograft biology and biomechanics. Cell Tissue Bank 2007;8:93–105.
14. Noah EM, Chen J, Jiao X, Heschel I, Pallua N. Impact of sterilization on the porous design and cell behavior in collagen sponges prepared for tissue engineering. Biomaterials 2002;23:2855–2861.
15. Jinno T, Miric A, Feighan J, Kirk SK Davy DT, Stevenson S. The effects of processing and low dose irradiation on cortical bone grafts. Clin Orthop Relat Res 2000;375:275–285.
16. Yunoki S, Marukawa E, Ikoma T, Sotome S, Fan H, Zhang X, Shinomiya K, Tanaka J. Effect of collagen fibril formation on bioresorbability of hydroxyapatite/collagen composites. J Mater Sci Mater Med 2007;18:2179–2183.
17. Yunoki S, Ikoma T, Monkawa A, Ohta K, Tanaka J, Sotome S, Shinomiya K. Influence of gamma irradiation on the mechanical strength and in vitro biodegradation of porous hydroxyapatite/collagen composite. J Am Ceram Soc 2006:89: 297–299.
18. Yunoki S, Ikoma T, Monkawa A, Marukawa E, Sotome S, Shinomiya K, Tanaka J. Three-dimensional porous hydroxyapatite/collagen composite with rubber-like elasticity. J Biomater Sci Polym Ed 2007;18:393–409.
19. Yunoki S, Ikoma T, Tsuchiya A, Monkawa A, Ohta K, Sotome S, Shinomiya K, Tanaka J. Fabrication and mechanical and tissue ingrowth properties of unidirectionally porous hydroxyapatite/collagen composite. J Biomed Mater Res B Appl Biomater 2007;80:166–173.
20. Schmitz JP, Schwartz Z, Hollinger JO, Boyan BD. Characterization of rat calvarial nonunion defects. Acta Anat 1990;138: 185–192.
21. Trombelli L, Farina R. Clinical outcomes with bioactive agents alone or in combination with grafting or guided tissue regeneration. J Clin Periodontol 2008;35(8Suppl):117–135; Review.
22. Donos N, Mardas N, Chadha V. Clinical outcomes of implants following lateral bone augmentation: Systematic assessment of available options (barrier membranes, bone grafts, split osteotomy). J Clin Periodontol 2008;35(8Suppl): 173–202;Review.

TISSUE ENGINEERING: Part A
Volume 16, Number 7, 2010

DOI: 10.1089/ten.tea.2009.0585

A Sustained Release of Lovastatin from Biodegradable, Elastomeric Polyurethane Scaffolds for Enhanced Bone Regeneration

Toshitaka Yoshii, M.D., Ph.D.,[1–3] Andrea E. Hafeman, M.S.,[2,4] Jeffry S. Nyman, Ph.D.,[1,2,5] Javier M. Esparza,[2] Kenichi Shinomiya, M.D., Ph.D.,[3] Dan M. Spengler, M.D.,[1] Gregory R. Mundy, M.D.,[1,2] Gloria E. Gutierrez, M.D.,[2] and Scott A. Guelcher, Ph.D.[2,4]

Scaffolds prepared from biodegradable polyurethanes (PUR) have been investigated as a supportive matrix and delivery system for skin, cardiovascular, and bone tissue engineering. In this study, we combined reactive two-component PUR scaffolds with lovastatin (LV), which has been reported to have a bone anabolic effect especially when delivered locally, for effective bone tissue regeneration. To incorporate LV into PUR scaffolds, LV was combined with the hardener component before scaffold synthesis. The PUR scaffolds containing LV (PUR/LV) demonstrated a highly porous structure with interconnected pores, which supported *in vitro* cell attachment and proliferation and *in vivo* osteoconductive potential. The PUR/LV scaffolds showed sustained release of biologically active LV, as evidenced by the fact that LV releasates significantly enhanced osteogenic differentiation of osteoblastic cells *in vitro*. A study of bone formation *in vivo* using a rat plug defect model showed that the PUR/LV scaffolds were biocompatible. Further, locally delivered LV enhanced new bone formation in the PUR scaffolds at week 4, while there were no obvious effects at week 2. These results suggest that the sustained LV delivery system from PUR scaffolds is a potentially safe and effective device for bone regeneration.

Introduction

THE CLINICAL NEED for bone reconstruction is increasing with the substantial rise in the elderly population.[1] While autologous bone grafts have been considered the most effective procedure for treating bone defects,[2] the usefulness of autograft is limited by its supply and operative morbidity.[3] These limitations necessitate the pursuit of alternatives. In the last 10 years, there have been tremendous advances in developing synthetic and biological scaffolds for bone tissue engineering.[4–6]

Scaffolds synthesized from biodegradable polyurethanes (PUR) have recently been investigated in several tissue engineering fields, including skin,[7–9] cardiovascular,[10,11] and bone.[12,13] In these applications, PUR scaffolds have been demonstrated to support cell in-growth and tissue remodeling. PUR scaffolds have also been shown to degrade to noncytotoxic decomposition products.[7,10,14–16] In addition to inherent flexibility in processing and tunable properties, the potential to inject them as a reactive two-component liquid is an attractive feature of these materials for noninvasive therapies.[9,13] PUR scaffolds have also been studied as a drug carrier for local delivery of signaling molecules, including basic fibroblast growth factor,[17] platelet-derived growth factor (PDGF),[8,9] and bone morphogenetic protein 2 (BMP2),[18] to accelerate tissue regeneration.

Statins, natural product compounds that inhibit 3-hydroxy-3-methylglutaryl-coenzyme A (HMG-CoA) reductase and reduce serum cholesterol, have recently been reported to have pleiotropic effects on various systems, including nervous, immune, cardiovascular, and skeletal systems.[19–21] For bone, statins have been shown to increase BMP2 expression and stimulate bone formation *in vivo* and *in vitro*.[22–26] In addition to the bone anabolic effect, another advantage of statins is their lower cost of synthesis compared to recombinant BMPs.[22] Further, statins have been safely used for years in treatment of hypercholesterolemia.[27,28] Therefore, the benefits of statins for treating bone injuries have increasingly generated interest among researchers and clinicians.[29–32]

[1]Department of Orthopaedics and Rehabilitation, and [2]Center for Bone Biology, Vanderbilt University Medical Center, Nashville, Tennessee.
[3]Section of Orthopaedic and Spinal Surgery, Graduate School, Tokyo Medical and Dental University, Tokyo, Japan.
[4]Department of Chemical and Biomolecular Engineering, Vanderbilt University, Nashville, Tennessee.
[5]Department of Veterans Affairs, Tennessee Valley Healthcare System, Nashville, Tennessee.

A major limitation in the clinical application of statins for bone regeneration is an appropriate delivery system. Statins are not effective enough in stimulating bone formation when given orally, because they are subject to first-pass metabolism in liver and thus do not reach sufficient concentrations at bone sites.[27] Therefore, local application of statins may be preferable for effective bone tissue repair. However, they disperse quickly and have short half-lives[22] when injected locally. Local application of statins with high doses may cause side effects, such as cytotoxicity or an adverse inflammatory response.[33,34] Therefore, a suitable delivery system is required to optimize their efficacy for bone regeneration.

In previous studies, Whang *et al.* demonstrated sustained release kinetics of simvastatin *in vitro* by grafting the statin to the hydrolytically degradable poly(lactide-*co*-glycolide).[35] Benoit *et al.* also synthesized a poly(ethylene glycol) (PEG) hydrogel-derived delivery system for fluvastatin and showed that the released fluvastatin induced osteogenic differentiation *in vitro*.[36] In other studies, Garrett *et al.* showed that locally delivered lovastatin (LV) from poly-(DL-lactide) nanoparticles (mean particle size ~200 nm) enhanced fracture repair.[37] Jeon *et al.* reported that controlled release of simvastatin hydroxyacid from microsphere composed of a blend of cellulose acetatephthalate and a poly(ethylene oxide) and poly(propyleneoxide) block copolymer enhanced bone formation in calvarial onlay model in rats.[38] However, release of statins from synthetic polymeric porous scaffolds for *in vivo* bone regeneration has yet to be investigated. In this study, we incorporated LV particles into PUR scaffolds using a reactive liquid molding process. We used PUR scaffolds as both a delivery system for LV in an active form for enhancing osteogenesis, and also to provide a suitable matrix for the newly formed bone. In a series of *in vitro* experiments, the release profile of LV, the biocompatibility of PUR scaffolds containing LV, and the osteogenic potential of LV released from PUR scaffolds were investigated. The effects of locally delivered LV from PUR scaffolds on *in vivo* bone formation were subsequently investigated in a rat femoral plug model.

Materials and Methods

Materials

Glycolide and D,L-lactide were obtained from Polysciences, tertiary amine catalyst (TEGOAMIN33) from Goldschmidt, and glucose from Acros Organics. Lysine triisocyanate (LTI) was purchased from Kyowa Hakko USA. LV was obtained from Stason Pharmaceuticals Incorporated, and α-minimal essential medium for cell culture was purchased from Fisher Scientific. All other reagents were purchased from Sigma-Aldrich.

Synthesis of PUR scaffolds

Trifunctional polyester polyols of 900-Da molecular weight were prepared from a glycerol starter; 60% ε-caprolactone, 30% glycolide, and 10% D,L-lactide monomers; and stannous octoate catalyst.[14,15] The components were mixed in a 100-mL reaction flask with mechanical stirring under argon for 36 h at 140°C, and the resulting polyol was subsequently washed with hexane and dried under vacuum at 80°C for 14 h. PUR scaffolds were synthesized by reactive liquid molding of LTI and a hardener comprising the polyol, 1.5 parts per hundred parts polyol (pphp) water, 1.5 pphp TEGOAMIN33 tertiary amine catalyst, 1.5 pphp sulfated castor oil stabilizer, and 4.0 pphp calcium stearate pore opener. The isocyanate was added to the hardener and mixed for 30 s in a Hauschild SpeedMixer™ DAC 150 FVZ-K vortex mixer (FlackTek, Inc.). The resulting reactive liquid mixture was allowed to rise freely for 10–20 min.[14,15] The targeted index (the ratio of NCO to OH equivalents times 100) was 115. Scanning electron microscopy (SEM; Hitachi S-4200 SEM) was utilized to observe the internal pore morphology of the PUR scaffolds. The pore size distribution was determined from SEM images of multiple PUR scaffold replicates.

Incorporation of LV in PUR scaffolds and in vitro release of LV

To incorporate LV into PUR scaffolds (PUR/LV scaffolds), LV particles were added to the hardener component before mixing with the isocyanate. Powdered LV was mixed thoroughly with the hardener at 20 μg (low dose) and 200 μg (high dose) per gram of foam. Triplicate scaffold samples were added to 5 mL each of phosphate-buffered saline (PBS), and LV was allowed to release over time at 37°C. At each time point, the release medium was collected and replaced with fresh PBS to approximate sink conditions. LV release was quantified daily from 1 to 30 days using high-performance liquid chromatography (Waters Breeze HPLC). Fifty microliters of each sample was filtered and injected into the HPLC. Releasates were passed through an XTerra reverse-phase guard column (C8 5-μm 3.9×20 mm) and XTerra reverse-phase column (C18 5-μm 4.6×250 mm) at a flow rate of 1.0 mL/min and analyzed at 237 nm. The mobile phases, at a ratio of 50/50 (A/B), were as follows: (1) 10 mM ammonium formate (pH 4.0) and isopropyl alcohol (95/5), and (2) 10 mM ammonium formate (pH 4.0) and acetonitrile (5/95). Both were filtered through a 0.2 μm filter and degassed under vacuum. The concentration of LV was calculated from peak area by injecting samples of known concentration and preparation of a standard curve correlating concentration with peak area.

In vitro biocompatibility of PUR/LV scaffolds

The *in vitro* biocompatibility of PUR and PUR/LV scaffolds was evaluated using MC3T3-E1 embryonic mouse osteoblast precursor cells. Considering that previous studies have demonstrated the *in vitro* biocompatibility of PUR scaffolds,[14,15] short-term studies (up to 5 days) were performed to determine whether the LV initially released from the scaffolds had any cytotoxic effects. MC3T3-E1 cells were statically seeded onto foam discs (9×1 mm) at 5×10^4 cells per well in 24-well tissue-culture polystyrene plates. Cells were cultured with α-minimal essential medium (Fisher Scientific) containing 10% fetal bovine serum (HyClone), and 1% penicillin/streptomycin (HyClone) at 37°C in a humidified incubator supplemented with 5% CO_2. The medium was changed every 2 days. After 5 days, the cell-seeded scaffolds were removed from culture, washed with PBS, and transferred to a new 24-well plate to verify cell adherence to the materials. About 4 μM calcein AM (Invitrogen–Molecular

Probes Live/Dead Viability/Cytotoxicity Kit) was added to the samples. Calcein AM dye is retained within live cells, imparting green fluorescence (excitation/emission: 495/515 nm). Cell viability was assessed qualitatively by fluorescent images acquired with an Olympus DP71 camera attached to a fluorescent microscope (Olympus CKX41, U-RFLT50).

In addition, cell attachment, viability, and proliferation were quantified using the MTT (3-[4,5-dimethylthiazol-2-yl]-2, 5-diphenyltetrazolium bromide) assay from Sigma-Aldrich.[39,40] For the attachment study, the samples were incubated for 4 h at 37°C with 5% CO_2 to allow the cells to attach to the scaffold after cell seeding. The same number of cells was plated on the polystyrene plates as a control, and cell attachment to the scaffolds was evaluated as a relative value to the control. For the viability/proliferation assay, the cells were cultured in the scaffolds for 2 and 5 days after seeding. The scaffolds were subsequently washed with PBS and transferred to a new 24-well plate. MTT solution was added to each well and incubated at 37°C for 4 h. The insoluble formazan crystals were dissolved in dimethyl sulfoxide, and the absorbance was measured at 590 nm in a microplate reader (ELX 800; Bio-Tek) with a reference wavelength at 620 nm.

Effect of LV delivery on osteogenic differentiation in vitro

The effects of LV released from PUR scaffolds (r-LV) on osteogenic differentiation were evaluated *in vitro* using MC3T3-E1 cells. Samples of released LV were obtained from the buffer in which the PUR/LV materials were incubated for the *in vitro* LV release assay; the concentration was adjusted by diluting in cell culture medium. MC3T3-E1 cells were treated with r-LV (1 μM) and fresh LV (1 μM) was used as a positive control. In general, since the concentrations of LV in the release samples were several orders of magnitude greater than the concentration needed for *in vitro* studies, the medium composition was not altered significantly. Osteogenic medium containing 2.5% fetal bovine serum, 5 mM β-glycerophosphate (Sigma-Aldrich), and 100 μg/mL ascorbic acid phosphate (Wako) was used for mineralization assays.

BMP2 expression. Cells were plated at 2×10^5 cells/well in six-well plates and treated with either r-LV or exogenous LV for 24 h ($n=4$). Total RNA was isolated using TriZOL reagent, and mRNA was transcribed to cDNA using Superscript II (Invitrogen). Quantitative PCR of mouse BMP2 mRNA was performed using the cDNA template and mouse BMP2 TaqMan primers/probe (Mm01340178_m1; Applied Biosystems) on the 7300 real-time PCR system (Applied Biosystems). Eukaryotic 18S rRNA detected using a VIC-MGB probe (4319413E; Applied Biosystems) served as an endogenous control.[41]

Alkaline phosphatase activity. Cells were plated at 2.5×10^4 cells/well in 48 wells and treated with either r-LV or exogenous LV for 3 and 7 days. Cells were washed with PBS and lysed with 0.1% Triton X-100. The plates were then subjected to three freeze–thaw cycles. The lysates (20 μL) were added to 100 μL of substrate buffer (2 mg/mL disodium *p*-nitrophenylphosphate hexahydrate and 0.75 M 2-amino-2-methyl-1-propanol). After incubation of the mixtures at 37°C for 30 min, absorbance at 405 nm was measured. Alkaline phosphatase activity (ALP) activity was determined from a standard curve generated by employing the reaction of a *p*-nitrophenyl solution. The ALP activity was normalized by the total protein content determined using the BCA assay (Pierce).

Mineralization assay. Cells were plated at 5×10^4 cells/well in 24 wells and treated with either r-LV or exogenous LV in the osteogenic medium for 25 days. After cells were washed with PBS and fixed with 10% phosphate-buffered formalin, mineralized nodule formation was evaluated by Von Kossa staining, wherein 5% silver nitrate solution was added to the well under incandescent light for 20–45 min. After granules developed, the silver nitrate was removed, and wells were washed with water to stop the reaction. Mineralized nodule formation was assessed by capture of digital images (4×) with an Olympus DP71 camera. The fractional area in the digital images taken from four regions per sample was evaluated using ImageJ software (NIH) and the average value calculated from $n=4$ replicates.

Effect of local LV delivery from PUR scaffolds on in vivo *bone formation*

Effect of local LV delivery from PUR scaffolds on bone formation *in vivo* was evaluated using a rat plug defect model.[42] All surgical procedures were reviewed and approved by the Institutional Animal Care and Use Committee. Male Sprague-Dawley rats (Harlan Labs) aged 8 weeks (200–250 g) were used for this study. A monocortical plug bone defect (3 mm) was created in the distal region of the femur diaphysis, and cylindrical PUR scaffolds (3×5 mm) were implanted into the defect. Treatment groups included PUR (without LV as a control), PUR/LV containing 100 μg LV (LV-H), and PUR/LV containing 25 μg of LV (LV-L) ($n=6$). After 2 and 4 weeks postimplantation, the rats were sacrificed, and the femurs removed and fixed in 10% phosphate-buffered formalin.

Quantitative 3D analysis of bone formation in the scaffolds was performed using a μCT40 (SCANCO Medical) at a voxel size of 24 mm (isotropic). The X-ray source settings were 55 kVp and 145 mA with an integration time of 300 ms. The region of interest (100 axial slices) was centered over the defect site in the distal femur. After reconstruction, the bone tissue was distinguished from air or soft tissue using a threshold of 270 per thousand (or 438.7 mgHA/cm^3), a Gaussian noise filter of 0.8, and support of 2. This threshold was consistent through all specimens. Utilizing Scanco evaluation software, the amount of bone formation in the scaffold was quantified as the ratio of bone volume per total volume, in which total volume was generated by measuring the contour of the defect site. Because the μCT40 is calibrated to known densities of hydroxyapatite (phantom), the mineral density (mgHA/cm^3) of each voxel was automatically provided for segmented bone. We evaluated the mean volumetric bone density of the mineralized tissue.

Rat bones were then decalcified with 10% ethylenediaminetetraacetic acid (Invitrogen), dehydrated, embedded in paraffin, and sectioned at 5 μm thickness. The coronal slice sections were stained with hematoxylin and eosin. Specimens were examined under light microscopy. For histomorphometric

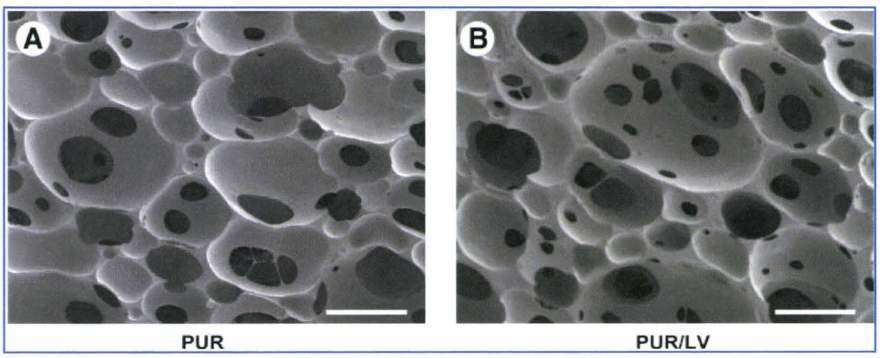

FIG. 1. Scanning electron microscope images. (**A**) Polyurethane (PUR) scaffolds and (**B**) PUR scaffolds incorporating lovastatin (PUR/LV: 200 μg LV/gram of foam). Scale bars: 250 μm.

examination, the amount of new bone formation in the scaffolds and the residual scaffolds were quantified at the center sections of the samples.[43] The newly formed bone and polymer scaffold remnants at the defect site were highlighted using image-editing software (Photoshop; Adobe Systems Incorporated) and measured using image-analysis software (Scion Image; Scioncorporation), and the ratio of new bone formation and implant per whole scaffold area was evaluated.

Statistics

Average values were expressed as the mean ± standard deviation. One-way analysis of variance and Bonferroni/Dunn *post hoc* test were used for statistical analysis. *p*-Values < 0.05 were considered significant.

Results

Synthesis of PUR scaffolds

Porous PUR scaffolds synthesized by reactive liquid molding exhibited porous structure as evidenced by SEM imaging (Fig. 1A). The pores were ellipsoidal, and the pore diameter was in the range of 200–500 μm. The thickness of the pore walls and struts was less than ~100 μm. The incorporation of LV did not obviously change the pore morphology (Fig. 1B); SEM images showed that PUR/LV (high dose) exhibited ellipsoidal pores in the same size range as the blank scaffold. Powdered LV incorporated in PUR scaffolds was not clearly visible in SEM images because of the small particle size compared to the thickness of the pore walls.

In vitro *release profile of LV from PUR scaffolds*

The amounts of LV released from PUR scaffolds *in vitro* were measured using HPLC and the cumulative% release of LV is shown in Figure 2. LV was released in a slow, sustained manner with a nearly linear release profile and a constant daily elution in both doses. Approximately 20% of LV was released from the scaffolds that contained high dose of LV in 30 days, and 10% of LV was released from the scaffolds with low dose of LV.

In vitro *biocompatibility of PUR/LV scaffolds*

Fluorescent micrographs of MC3T3-E1 osteoblastic cells cultured on PUR/LV scaffolds after 5 days are shown in Figure 3A–C. The green viable cells, as indicated by dye uptake, were easily distinguished from the autofluorescent scaffold material. The osteoblastic cells infiltrated the porous structure of the scaffold and adhered to the pore walls in all three treatment groups.

An MTT assay was also performed to quantify osteoblastic cell attachment, viability, and proliferation on the scaffolds. There were no significant differences among the treatment groups in the attachment of cells to the scaffolds after 4 h of incubation (Fig. 3D). When the cells were cultured on the scaffolds for 2 and 5 days, the MTT assay showed that the number of cells substantially increased from day 2 to 5, suggesting that the cells proliferated in all three materials (Fig. 3E). There were no differences among the treatment groups in the number of viable cells at each time point. These results suggest that PUR scaffolds are biocompatible and the incorporation of LV did not affect cell viability or proliferation on the scaffolds in osteoblastic cell culture.

Effect of LV delivery on osteogenic differentiation in vitro

To verify the bioactivity of released LV from PUR scaffolds, the effects of released LV on *BMP2* gene expression and osteoblastic differentiation were examined in monolayer culture of MC3T3-E1 osteoblastic cells. Cells were cultured with released LV on tissue culture polystyrene, rather than directly on PUR/LV scaffolds, since LV release rates *in vitro* were not be sufficiently high at this experimental timescale to initiate the biological effect of LV. As shown in Figure 4A,

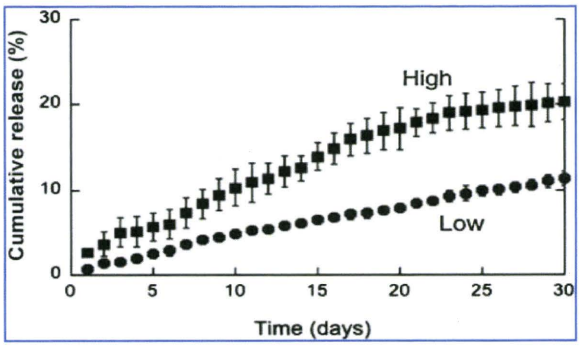

FIG. 2. *In vitro* release kinetics of LV delivered from PUR scaffolds. Cumulative percent release from PUR incorporating LV at 20 μg (Low) and 200 μg (High) per gram of foam.